ChemPubSoc Europe

DOI: 10.1002/chem.201406485

CHEMISTRY
A European Journal
Full Paper

Metal–Oxo Species

Characterization and Reactivity of a Terminal Nickel(III)–Oxygen Adduct

Paolo Pirovano,[a] Erik R. Farquhar,[b] Marcel Swart,[c] Anthony J. Fitzpatrick,[d]
Grace G. Morgan,[d] and Aidan R. McDonald*[a]

Abstract: High-valent terminal metal–oxygen adducts are hypothesized to be the potent oxidizing reactants in late transition metal oxidation catalysis. In particular, examples of high-valent terminal nickel–oxygen adducts are scarce, meaning there is a dearth in the understanding of such oxidants. A monoanionic Ni^{II}-bicarbonate complex has been found to react in a 1:1 ratio with the one-electron oxidant tris(4-bromophenyl)ammoniumyl hexachloroantimonate, yielding a thermally unstable intermediate in high yield (ca. 95%). Electronic absorption, electronic paramagnetic resonance, and X-ray absorption spectroscopies and density functional theory calculations confirm its description as a low-spin ($S=\frac{1}{2}$), square planar Ni^{III}–oxygen adduct. This rare example of a high-valent terminal nickel–oxygen complex performs oxidations of organic substrates, including 2,6-di-*tert*-butylphenol and triphenylphosphine, which are indicative of hydrogen atom abstraction and oxygen atom transfer reactivity, respectively.

Introduction

Nature employs Fe- and Cu-containing oxygenases to perform hydrocarbon oxidation and Mn-containing photosystem II to perform water oxidation.[1] Similarly, many synthetic Mn-, Fe-, Co-, Ni-, and Cu-containing catalysts are capable of both hydrocarbon and water oxidation.[2] In most of these natural and non-natural first-row transition metal-catalyzed conversions, terminal high-valent metal–oxygen adducts, such as metal–oxo (M=O), metal–oxyl (M–O·) or metal–hydroxo (M–OH) intermediates, have been implicated as the reactive oxidants. These oxidants are potent hydrogen atom abstraction (HAA) or oxygen atom transfer (OAT) reagents, capable of activating some of the most inert of substrates. Many examples of enzymatic and synthetic terminal oxomanganese and oxoiron species have arisen in the past ten years;[3] however there remains a dearth in the number of terminal late transition metal–oxygen adducts (metal = Co, Ni, Cu). The groups of Ray/Nam, and Tolman have recently made great strides in preparing the first examples of scandium(III) oxocobalt(IV) and hydroxocopper(III) species, respectively.[4] However, well-characterized high-valent terminal nickel–oxygen adducts remain elusive.

Synthetic nickel-containing complexes have been exploited as catalysts for the oxidation of hydrocarbons[5] and water.[6] Similarly, nickel-containing films and nanoparticles have been employed as oxidation catalysts.[2b,7] Terminal high-valent nickel–oxygen adducts ($Ni^{III/IV}$–OX) have been postulated as the active oxidant in these systems. However, very few such species have been isolated and well-characterized to date.[5,8] Interestingly, computational studies have forecast that a Ni^{III}=O species would be capable of the activation of the strongest of C–H bonds (CH_4, bond dissociation energy (BDE) = 104 kcal mol^{-1}).[9]

Several groups have attempted to prepare high-valent nickel–oxygen adducts; for example Ray and co-workers reported that the oxidation of [Ni^{II}(TMG_3tren)(OTf)](OTf) (TMG_3tren = (tris[2-(*N*-tetramethylguanidyl)ethyl]amine, OTf = trifluoromethanesulfonate) with 3-chloroperoxybenzoic acid produced two species claimed to be Ni^{III}–O(X) complexes.[10] However, the low yield (15%) of Ni^{III} and identification of at least two Ni^{III} species in the reaction mixture hampered their characterization. Chmielewski and Latos-Grażyński treated a Ni^{III}–Br complex with hydroxide to yield a new species that was claimed to be a Ni^{III}–OH complex.[11] However, this species was only characterized by EPR spectroscopy, and no reactivity studies were performed. Chiou and Liaw prepared Ni^{III}–OR (R = Me, Ph) species, but did not report on their HAA or OAT reactivity properties.[12] Interestingly, several μ-oxo–dinickel(III)[13] and nickel-containing heterobimetallic μ-oxo complexes[14]

---

[a] P. Pirovano, Dr. A. R. McDonald
School of Chemistry and CRANN/AMBER Nanoscience Institute
The University of Dublin, Trinity College
College Green, Dublin 2 (Ireland)
E-mail: aidan.mcdonald@tcd.ie

[b] Dr. E. R. Farquhar
Case Western Reserve University Center for Synchrotron Biosciences
National Synchrotron Light Source, Brookhaven National Laboratory
Upton, NY 11973 (USA)

[c] Prof. M. Swart
Institut de Química Computacional i Catàlisi
Universitat de Girona, Facultat de Ciències
Campus Montilivi, 17071 Girona, Catalunya (Spain)

[d] A. J. Fitzpatrick, Dr. G. G. Morgan
School of Chemistry and Chemical Biology
University College Dublin, Science Centre
Belfield, Dublin 4 (Ireland)

Supporting information for this article is available on the WWW under http://dx.doi.org/10.1002/chem.201406485.

have been isolated and found to be effective HAA reagents. In contrast, there remains a lack of suitable high-valent terminal nickel–oxygen adducts that could help us understand further the reactivity properties of late transition metal oxidants. With this in mind, we set out to prepare, characterize, and investigate the reactivity of such complexes. We identified Holm's $[Ni^{II}(OH)(pyN_2^{Me_2})]^-$ (**1**; Scheme 1) and $[Ni^{II}(OCO_2H)(pyN_2^{Me_2})]^-$ (**2**; Scheme 1) complexes ($pyN_2^{Me_2}$ = *N*,*N*′-bis(2,6-dimethylphenyl)-2,6-pyridinedicarboxamidate) as excellent candidates for the generation of high-valent terminal nickel–oxygen adducts.[15] Using similar 2,6-pyridinedicarboxamidate ligands, thermally stable Ni^{III} and Ni^{IV} complexes,[16] as well as Cu^{II}–superoxide,[17] and Cu^{III}–OH[4c,18] entities have been isolated. Herein, we describe the oxidation of **2** (which is formed from the reaction between **1** and CO_2; Scheme 1), to yield a metastable Ni^{III}–O(X) species that displays the ability to perform HAA and OAT.

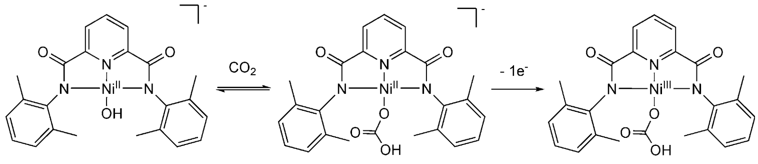

1 **2** **3**

Scheme 1. Complexes **1**,[15a] **2**,[15a] and **3**. Schematic representation of the preparation of **2** and **3**.

Results and Discussion

In acetone, at −80 °C, **2** was treated with the organic oxidant tris(4-bromophenyl)ammoniumyl hexachloroantimonate[19] ("Magic Blue", dissolved in CH_3CN, $E^{\circ\prime} = 0.70$ V vs. Fc^+/Fc[20]). An instantaneous reaction took place, as evidenced by the appearance of two intense features in the electronic absorption spectrum ($\lambda_{max} = 520$ and 790 nm; Figure 1), assigned to a novel species **3**. A titration of Magic Blue against **1** showed that the intensity of the new features reached a maximum after the addition of one equivalent of Magic Blue (Figure 1, inset). The addition of greater than one equivalent of Magic Blue did not cause a further change in the new features, while the presence of excess unreacted Magic Blue in the reaction mixture was observed in the electronic absorption spectrum (Figure S1 in the Supporting Information). Initial indications thus suggested that **2** had been oxidized by one electron yielding a novel species, **3**, that we postulate is a Ni^{III}–OCO_2H complex.

The intense absorption features in the visible and near-IR (NIR) regions of the UV/Vis spectrum, observed upon the reaction between **2** and Magic Blue to yield **3**, suggest a change in the oxidation state of the Ni center. Many of the Ni^{III} complexes reported to date display similarly intense chromophores in the visible and NIR regions of their absorption spectra.[10,12,16,21] Intermediate **3** could be generated in acetone or THF. The features associated with **3** are the same in both solvents. Likewise, when **3** was prepared in the presence or absence of excess CH_3CN (acetone or CH_3CN can be used as the solvent for Magic Blue) no difference in the electronic absorption features was noted. These observations are important as they demonstrate that solvent is not coordinating to the Ni^{III} center in **3**. Should solvent coordinate to the Ni^{III} center in **3**, one would anticipate different UV/Vis characteristics of the oxidized product in different solvent media.

3 was further characterized using X-band electron paramagnetic resonance (EPR) spectroscopy. An acetone solution of **3** was frozen in liquid nitrogen and an axial spectrum was obtained at 113 K (Figure 2, $g = 2.25$, 2.02). The yield of Ni^{III} was calculated to be 95 % (±15 %) by double integration of the signal of **3** against that of a radical standard (TEMPO = (2,2,6,6-tetramethylpiperidin-1-yl)oxyl)). The obtained g values are consistent with an $S = {}^1\!/_2$ (low-spin) d^7 Ni^{III} species,[21d,22] and the average g value ($g_{av.} = 2.17$) is indicative of the unpaired electron sitting on the Ni center, rather than being a ligand-based radical. Importantly, $g\perp >> g_{||}$, which is typical for axially elongated octahedral complexes or square planar complexes.[21b,d,22,23]

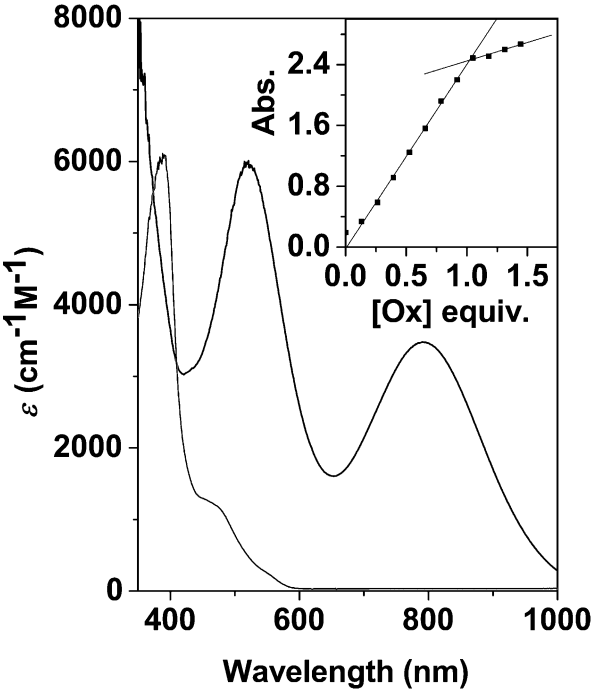

Figure 1. UV/Vis spectrum of **2** (grey trace, 0.4 mM in acetone) that was treated with Magic Blue at −80 °C to yield 3 (black trace). Inset: Titration of Magic Blue with **2**, monitored by plotting the intensity of the $\lambda_{max} = 520$ nm feature versus equivalents of Magic Blue.

The most likely configurations for a low-spin d^7 ion in pseudo-tetragonal symmetry involve the unpaired electron density being located in an orbital of predominant d_{z^2} or d_{xy} character. Instances where $g\perp >> g_{||}$ have been usually understood to correspond to a d_{z^2} singly-occupied orbital.[21b,d,22,23b,d] Overall, the EPR analysis suggests that oxidation of the square-planar precursor **2** resulted in the loss of an elec-

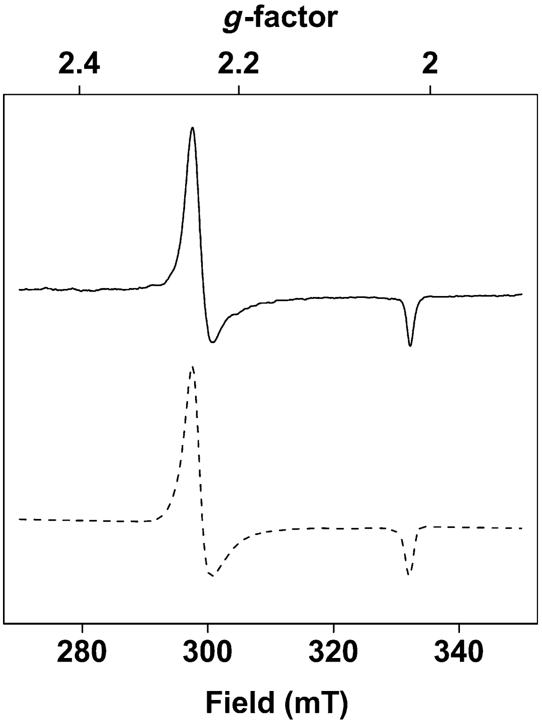

Figure 2. Solid trace: X-band EPR spectrum of **3** in a frozen acetone solution. Measured at 113 K; microwave power = 31.6 mW; modulation amplitude = 0.5 mT; $g\perp = 2.25$, $g_{||} = 2.02$, $g_{av.} = 2.17$. Dashed trace: simulated spectrum for **3**. The system was modelled as an $S = {}^1\!/_2$ electron spin with axial g tensor and inhomogeneous line broadening. The greater line broadening in the x and y directions is possibly due to unresolved hyperfine coupling with the ^{14}N nuclei of the ligand.

tron yielding a square-planar $S = {}^1\!/_2$ d^7 Ni^{III} species, **3**, with a metal-based d_{z^2}-like occupied orbital. Density functional theory (DFT) Mulliken spin density calculations were performed, in order to further probe the location of the unpaired electron density in **3**. These calculations supported the experimental observations that the unpaired spin predominantly resides in a metal-based molecular orbital. The DFT calculations predict that either metal-based d_{z^2}- or d_{xy}-like molecular orbitals are the likely locations of the unpaired electron density (Figure 3 displays spin density plot for d_{z^2} occupancy). The DFT calculations thus support the EPR-determined electronic structure of **3**.

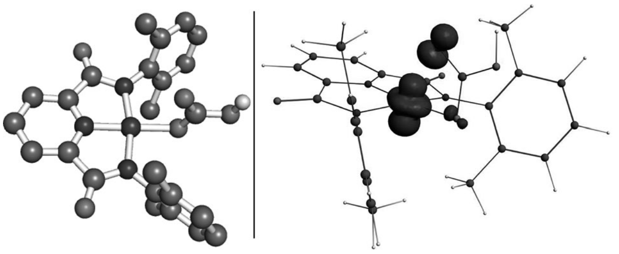

Figure 3. Left: DFT-optimized structure of **3**. Hydrogen atoms (except bicarbonate proton) have been excluded for clarity. Right: DFT-optimized spin density plot of **3**.

X-ray absorption spectroscopy (XAS) was employed to analyze the electronic and structural properties of **3**. The XAS edge energy measured for **3** (8345 eV) lies in the expected range for Ni^{III} complexes.[14,24] Interestingly, there is only a very minor shift in the K-edge energy compared to the K-edge energy measured for Ni^{II}-containing **2** (Figure 4). This is not unusual for Ni (and indeed Cu) K-edge analysis; several groups have made similar observations when comparing Ni$^{II/III}$ species within comparable coordination environments.[24a,25] Contributions to the edge from 1s→4p absorption features distort the edge and prevent accurate assessment of the edge shift upon oxidation of **2** to yield **3**. The derivatives of the normalized X-ray absorption near-edge spectrum (XANES) indicate a modest edge shift of 0.1–0.2 eV when comparing the 1s→3d pre-edge transition of **2** to **3**, in accordance with an increased oxidation state of the Ni center in **3**. Although there appears to be negligible change in the edge energy between **2** and **3**, the shape of the edge and relative intensities of features in the edge are markedly different. Such differences are indicative of the distinct electronic environments of the Ni-center in complexes **2** and **3**.

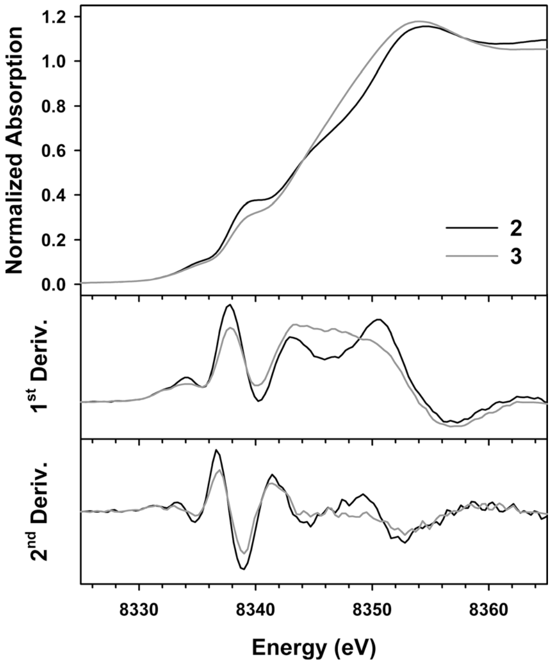

Figure 4. XANES spectra of **2** (black trace) and **3** (grey trace), along with associated first and second derivatives.

Extended X-ray absorption fine structure (EXAFS) analysis of **3** yielded a disordered first coordination shell of 4 O/N donors (see the Supporting Information, Figure S2 and Table S1). This shell could be split into two components with two scatterers at approximately 1.84 Å and two scatterers at approximately 1.99 Å giving the best fit of the experimental data obtained for **3** (Table 1). These observations suggest that a single-bonded oxygen ligand is present in **3**, that is, that the bicarbonate remains intact. Attempts to fit the data containing a very short

Table 1. Nickel–ligand bond distances for **2** and **3**.

	Ni–OCO_2H	Ni–N(py)	Ni–N(amid)
2[a][15a]	1.871	1.817	2@1.895
2[b]	4@1.87		
2[c]	1.90	1.80	2@1.90
3[b]	2@1.84		2@1.99
3[c]	1.96	1.84	2@1.93

[a] Determined using XRD; [b] determined using EXAFS; [c] determined using DFT.

Ni–O bond (ca. 1.65 Å) resulted in very poor fits, ruling out the possibility of **3** being a Ni^{III}=O species. Comparison of the EXAFS fits for **2** and **3** suggests there are little to no structural differences in the two complexes. The fits acquired for **2** match well with the X-ray diffraction determined bond distances obtained for **2**.[15a] We have employed DFT to further understand the structural properties of **3** (Table 1, Figure 3). The DFT predictions indicate that the bicarbonate ligand in **3** would remain bound in a monodentate fashion, in good agreement with the EXAFS analyses of a first coordination sphere of four donors. Furthermore, the computational analyses predicted that the d^7 Ni^{III} ion in **3** would remain in a square planar coordination environment analogous to that seen for **2**, in good agreement with the EPR measurements that indicate the Ni^{III} ion sits in a square planar environment. DFT also predicted that the Ni–OCO_2H and Ni–N(py) bond distances in **3** would be 1.96 Å and 1.84 Å (Table 1), respectively, in reasonably good agreement with the EXAFS analyses showing two O/N scatterers at approximately 1.84 Å. The combination of EXAFS and DFT predictions shows that the Ni center in **3** has remained 4-coordinate, in a square planar environment, and that the bicarbonate ligand is present.

It is important to note that the obtained EXAFS data could also be reasonably well fit with an OH ligand (in place of OCO_2H). Holm and co-workers demonstrated that **2** reversibly binds CO_2, and it is reasonable to suggest the affinity of **3** for CO_2 may be less than for **2**.[15a,b,d] We endeavored to probe **3** using Raman spectroscopy, but failed to identify peaks that confirmed the presence of either OH or OCO_2H ligands. We were hampered by the rich Raman spectrum of the acetone support medium. We also failed in our efforts to obtain mass spectrometric evidence for the molecular formula of **3**, presumably as a result of the low thermal stability of **3**. It is important to note that oxidation of **1** with Magic Blue does not yield the same spectroscopic features attributed to **3**, but in fact yields an as yet unidentified species. We therefore conclude that **3** retains the coordinated OCO_2H ligand.

Compound **3** was stable at $-80\,^{\circ}C$, but decayed upon warming above $-40\,^{\circ}C$. After thermal decay and acidic workup of the reaction mixture, the protonated ligand ($H_2pyN_2^{Me_2}$) was recovered without any indications of ligand oxidation (no evidence for ligand hydroxylation or oxidative decomposition was obtained by mass spectrometry or ^1H NMR spectroscopy). Interestingly, ESI-MS showed the presence of trace amounts of hydroxyacetone, pyruvic acid, and acetic acid.[26] Importantly, at $-40\,^{\circ}C$, the half-life of **3** in [H_6]acetone was 5600 s, whereas in [D_6]acetone it was found to be 6800 s (kinetic isotope effect (KIE) = 1.2). The observation of such acetone-derived products and an extended lifetime in perdeuterated solvent supports the postulate that **3** oxidizes acetone by rate-limiting HAA during its thermal decay. This is an important discovery, as acetone contains a very strong C–H bond (BDE = 93 $kcal\,mol^{-1}$)[27], suggesting that **3** is a very capable oxidant.

We investigated further the HAA reactivity of **3** towards external substrates by its reaction with molecules containing somewhat weaker X–H bonds (X = C, O; we were limited in our substrate scope by solubility issues at low temperature). At $-40\,^{\circ}C$, **3** reacted with 100 equivalents of 2,6-di-*tert*-butylphenol (DTBP), as evidenced by the disappearance (600 s) of the electronic absorption features attributed to **3** (see the Supporting Information, Figure S3). This resulted in the appearance of a new band at $\lambda_{max} = 555$ nm, which we attribute to the formation of the phenoxyl radical as a result of HAA from DTBP by **3**.[28] EPR spectroscopy confirmed the formation of a phenoxyl radical (see the Supporting Information, Figure S4). After warming to room temperature, 3,3′,5,5′-tetra-*tert*-butyl-[1,1′-bis(cyclohexane)]-2,2′,5,5′-tetraene-4,4′-dione (see the Supporting Information, Scheme S1) and traces of 2,6-di-*tert*-butylquinone were detected by GC-MS. These products are formed by radical coupling or thermal decomposition, respectively, of the parent 2,6-di-*tert*-butylphenoxyl radical. A pseudo-first-order rate constant (k_{obs}) for this reaction was determined by plotting the change in absorbance features for **3** against time and fitting the resulting curve (see the Supporting Information, Figure S5). A second-order rate constant (k_2) was calculated from the slope of a linear plot of k_{obs} values determined under a series of substrate concentrations (see the Supporting Information, Figure S6). The k_2 value determined for the reaction between **3** and DTBP was $0.1040\,M^{-1}\,s^{-1}$, whereas for deutero-DTBP a k_2 value of $0.0503\,M^{-1}\,s^{-1}$ was determined, yielding a KIE value of 2.1. This KIE value is consistent with **3** performing HAA on the DTBP O–H bond, and with HAA being rate-limiting.

Compound **3** was also found to react with 1-benzyl-1,4-dihydronicotinamide (BNAH; C–H bond dissociation energy (BDE = 64 $kcal\,mol^{-1}$)) at $-80\,^{\circ}C$, as evidenced by a rapid disappearance of the visible absorption features attributed to **3** (see the Supporting Information, Figure S7). The product of this reaction was identified by ^1H NMR as 1-benzyl-1-pyridinium-3-carboxamide, which typically forms as a result of HAA from the C–H bond of BNAH. This product formed as a result of a two-electron oxidation of BNAH. We assume this occurs through initial HAA from BNAH followed by an electron transfer from the resultant product to another molecule of **3**. In summary, **3** was found to be a quite reactive HAA reagent capable of activating O–H and C–H bonds at low temperatures.

We also probed the capacity of **3** to carry out OAT. **3** was treated with triphenylphosphine (PPh_3, 50 equiv) at $-80\,^{\circ}C$, resulting in the formation of triphenylphosphine oxide ($O{=}PPh_3$, detected by ESI-MS and ^{31}P NMR spectroscopy) in near quantitative yields (see the Supporting Information, Figure S8). OAT is a two-electron transfer process; thus the formation of $O{=}PPh_3$ from this reaction would be expected to yield a Ni^I product.

We did not observe any Ni^I species, but rather only Ni^{II} products. Presumably, the formed Ni^I product reacted with another molecule of **3** (similar to the BNAH oxidation) to yield the observed Ni^{II} products. Interestingly, **3** was completely consumed by just 0.5 equivalents of PPh_3 and BNAH, confirming our suspicions about the mechanisms of its reductive decay. A second-order rate constant (k_2) for the reaction between **3** and PPh_3 was determined ($5.3\,\text{M}^{-1}\,\text{s}^{-1}$; see the Supporting Information, Figures S9 and S10). This k_2 value for PPh_3 oxidation is quite high compared to values determined for Fe=O and Mn=O complexes in the same reaction.[29] We believe it is quite significant that the Ni species displayed such a high rate constant. **3** was also found to be highly reactive towards one-electron reductants. Ferrocene (1 equiv in acetone) reacted with **3** instantaneously at −80 °C, as evidenced by the disappearance of UV/Vis features attributed to **3**, and the formation of new features in the visible region that can be attributed to the ferrocenium cation ($\lambda_{max}=630$ nm; see the Supporting Information, Figure S11). The conversion of ferrocene to ferrocenium was quantitative and the yield of ferrocenium was determined to correspond to exactly one equivalent of **3** being reduced. **3** thus represents an exciting example of a terminal nickel–oxygen adduct that is capable of HAA, OAT, and electron transfer.

Conclusion

In summary, the one-electron oxidation of **2** at low temperature generates a Ni^{III} complex, **3**. EPR spectroscopy suggested the oxidation was borne principally by the central metal atom, yielding a low-spin d^7 Ni^{III} ion in a square planar coordination environment. XAS analysis provided further support for this, indicating that **3** contained a Ni^{III} center coordinated by four N/O donor ligands. DFT calculations on the structure and Mulliken spin density further supported these experimental conclusions. **3** was capable of oxidizing organic substrates including acetone, DTBP, BNAH, and PPh_3. This constitutes the first example of a terminal Ni^{III}–O(X) species that is sufficiently well-behaved to allow thorough structural, spectroscopic, and reactivity investigations. This is an important step towards the elucidation of the properties of these compounds and their role in oxidation catalysis.

Experimental Section

1 was prepared according to the reported procedure[15a] and recrystallized from DMF/diethyl ether. Solutions of **2** were obtained by exposing **1** to CO_2, according to the reported procedures,[15a] and they were either used directly or the compound was isolated by crystallization. Deutero-2,6-di-*tert*-butylphenol was prepared according to a modification of the reported literature procedure (see the Supporting Information).[29]

Preparation of 3

A 0.4 mM solution of **2** in acetone was cooled in a cuvette to −80 °C. A freshly prepared 15 M solution of Magic Blue in acetonitrile (52 μL) was added under continuous stirring. The formation of **3** was immediate, as evidenced by the formation of bands in the UV/Vis spectrum at 520 and 790 nm.

General procedure for reactivity experiments

A solution of **3** at −80 °C (or −40 °C) was prepared according to the above procedure. Substrates were added as concentrated acetone solutions. The reactions were monitored using UV/Vis spectroscopy, and after complete disappearance of the features corresponding to **3**, were allowed to warm up to room temperature. The reaction mixtures were diluted with methanol for MS analysis, or the solvent was removed in vacuo for NMR analysis.

Rate constants determination

Reactions were carried out with 7 to 300 equivalents of substrate to ensure pseudo-first-order conditions. The second-order rate constant (k_2) was determined from the linear dependence of the pseudo-first-order rate constant (k_{obs}) on substrate concentration. Values for the observed k_{obs} were obtained by fitting the decay of the absorbance at 520 nm during a reaction as an exponential. The average from repeated experiments were utilized for the determination of k_2.

Additional experimental, spectroscopic, and computational information is included in the supporting information file. This includes [D_6]acetone NMRs of **1** and **2**, EPR and XAS methods and data analysis, DFT methods and optimized-structures coordinates, spectra and kinetic data for the reactivity studies.

Acknowledgements

This publication has emanated from research supported in part by the European Union (FP7–333948, AMcD), a research grant from Science Foundation Ireland (SFI/12/RC/2278, AMcD), and COST Action CM1305 (ECOSTBio). M.S. acknowledges MINECO (CTQ2011–25086/BQU), DIUE of the Generalitat de Catalunya (2014SGR1202), MICINN (Ministry of Science and Innovation, Spain), the FEDER fund (UNGI08–4E-003) and CESCA. Operation of NSLS X3B is supported by NIH grant P30-EB-009998. The NSLS is supported by the U.S. Department of Energy, Office of Science, Office of Basic Energy Sciences, under contract no. DE-AC02–98CH10886.

Keywords: high-valent metals · metal–oxo species · nickel · oxidation catalysis · reactive intermediates

[1] a) M. Sono, M. P. Roach, E. D. Coulter, J. H. Dawson, *Chem. Rev.* **1996**, *96*, 2841 – 2888; b) I. G. Denisov, T. M. Makris, S. G. Sligar, I. Schlichting, *Chem. Rev.* **2005**, *105*, 2253 – 2277; c) E. I. Solomon, T. C. Brunold, M. I. Davis, J. N. Kemsley, S.-K. Lee, N. Lehnert, F. Neese, A. J. Skulan, Y.-S. Yang, J. Zhou, *Chem. Rev.* **2000**, *100*, 235 – 350; d) M. Costas, M. P. Mehn, M. P. Jensen, L. Que, *Chem. Rev.* **2004**, *104*, 939 – 986; e) E. I. Solomon, D. E. Heppner, E. M. Johnston, J. W. Ginsbach, J. Cirera, M. Qayyum, M. T. Kieber-Emmons, C. H. Kjaergaard, R. G. Hadt, L. Tian, *Chem. Rev.* **2014**, *114*, 3659 – 3853; f) J. Yano, V. Yachandra, *Chem. Rev.* **2014**, *114*, 4175 – 4205.

[2] a) T. Punniyamurthy, S. Velusamy, J. Iqbal, *Chem. Rev.* **2005**, *105*, 2329 – 2363; b) A. Singh, L. Spiccia, *Coord. Chem. Rev.* **2013**, *257*, 2607 – 2622.

[3] a) W. Nam, *Acc. Chem. Res.* **2007**, *40*, 522 – 531; b) C. Krebs, D. Galonić Fujimori, C. T. Walsh, J. M. Bollinger, *Acc. Chem. Res.* **2007**, *40*, 484 – 492; c) L. Que, *Acc. Chem. Res.* **2007**, *40*, 493 – 500; d) G. Yin, *Coord. Chem. Rev.* **2010**, *254*, 1826 – 1842; e) A. R. McDonald, L. Que, *Coord. Chem. Rev.*

2013, *257*, 414–428; f) W. J. Song, M. S. Seo, S. D. George, T. Ohta, R. Song, M.-J. Kang, T. Tosha, T. Kitagawa, E. I. Solomon, W. Nam, *J. Am. Chem. Soc.* **2007**, *129*, 1268–1277; g) X. Wu, M. S. Seo, K. M. Davis, Y.-M. Lee, J. Chen, K.-B. Cho, Y. N. Pushkar, W. Nam, *J. Am. Chem. Soc.* **2011**, *133*, 20088–20091; h) T. Taguchi, R. Gupta, B. Lassalle-Kaiser, D. W. Boyce, V. K. Yachandra, W. B. Tolman, J. Yano, M. P. Hendrich, A. S. Borovik, *J. Am. Chem. Soc.* **2012**, *134*, 1996–1999.

[4] a) F. F. Pfaff, S. Kundu, M. Risch, S. Pandian, F. Heims, I. Pryjomska-Ray, P. Haack, R. Metzinger, E. Bill, H. Dau, P. Comba, K. Ray, *Angew. Chem. Int. Ed.* **2011**, *50*, 1711–1715; *Angew. Chem.* **2011**, *123*, 1749–1753; b) S. Hong, F. F. Pfaff, E. Kwon, Y. Wang, M.-S. Seo, E. Bill, K. Ray, W. Nam, *Angew. Chem. Int. Ed.* **2014**, *53*, 10403–10407; *Angew. Chem.* **2014**, *126*, 10571–10575; c) P. J. Donoghue, J. Tehranchi, C. J. Cramer, R. Sarangi, E. I. Solomon, W. B. Tolman, *J. Am. Chem. Soc.* **2011**, *133*, 17602–17605.

[5] a) J. D. Koola, J. K. Kochi, *Inorg. Chem.* **1987**, *26*, 908–916; b) R. Irie, Y. Ito, T. Katsuki, *Tetrahedron Lett.* **1991**, *32*, 6891–6894; c) T. Yamada, T. Takai, O. Rhode, T. Mukaiyama, *Chem. Lett.* **1991**, *20*, 1–4; d) R. I. Kureshy, N. H. Khan, S. H. R. Abdi, P. Iyer, A. K. Bhatt, *J. Mol. Catal. A* **1998**, *130*, 41–50; e) I. Fernández, J. Pedro, A. L. Rosello, R. Ruiz, X. Ottenwaelder, Y. Journaux, *Tetrahedron Lett.* **1998**, *39*, 2869–2872; f) T. Nagataki, Y. Tachi, S. Itoh, *Chem. Commun.* **2006**, 4016–4018; g) T. Nagataki, S. Itoh, *Chem. Lett.* **2007**, *36*, 748–749; h) T. Nagataki, K. Ishii, Y. Tachi, S. Itoh, *Dalton Trans.* **2007**, 1120–1128; i) M. Balamurugan, R. Mayilmurugan, E. Suresh, M. Palaniandavar, *Dalton Trans.* **2011**, *40*, 9413–9424; j) M. Sankaralingam, P. Vadivelu, E. Suresh, M. Palaniandavar, *Inorg. Chim. Acta* **2013**, *407*, 98–107.

[6] a) G. Zhu, E. N. Glass, C. Zhao, H. Lv, J. W. Vickers, Y. V. Geletii, D. G. Musaev, J. Song, C. L. Hill, *Dalton Trans.* **2012**, *41*, 13043–13049; b) M. Zhang, M.-T. Zhang, C. Hou, Z.-F. Ke, T.-B. Lu, *Angew. Chem. Int. Ed.* **2014**, *53*, 13042–13048; *Angew. Chem.* **2014**, *126*, 13258–13264.

[7] a) G. Chen, L. Chen, S.-M. Ng, T.-C. Lau, *ChemSusChem* **2014**, *7*, 127–134; b) A. Singh, S. L. Y. Chang, R. K. Hocking, U. Bach, L. Spiccia, *Catal. Sci. Technol.* **2013**, *3*, 1725–1732; c) D. Hong, Y. Yamada, T. Nagatomi, Y. Takai, S. Fukuzumi, *J. Am. Chem. Soc.* **2012**, *134*, 19572–19575; d) M. Dincă, Y. Surendranath, D. G. Nocera, *Proc. Natl. Acad. Sci. USA* **2010**, *107*, 10337–10341; e) P. Boizumault-Moriceau, *Appl. Catal. A* **2003**, *245*, 55–67; f) X. Zhang, J. Liu, Y. Jing, Y. Xie, *Appl. Catal. A* **2003**, *240*, 143–150.

[8] a) M. Sankaralingam, M. Balamurugan, M. Palaniandavar, P. Vadivelu, C. H. Suresh, *Chem. Eur. J.* **2014**, *20*, 11346–11361; b) J. F. Kinneary, J. S. Albert, C. J. Burrows, *J. Am. Chem. Soc.* **1988**, *110*, 6124–6129; c) H. Yoon, T. R. Wagler, K. J. O'Connor, C. J. Burrows, *J. Am. Chem. Soc.* **1990**, *112*, 4568–4570; d) D. K. Bediako, Y. Surendranath, D. G. Nocera, *J. Am. Chem. Soc.* **2013**, *135*, 3662–3674.

[9] A. W. Pierpont, T. R. Cundari, *Inorg. Chem.* **2010**, *49*, 2038–2046.

[10] F. F. Pfaff, F. Heims, S. Kundu, S. Mebs, K. Ray, *Chem. Commun.* **2012**, *48*, 3730–3732.

[11] P. J. Chmielewski, L. Latos-Grażyński, *Inorg. Chem.* **1997**, *36*, 840–845.

[12] T.-W. Chiou, W.-F. Liaw, *Inorg. Chem.* **2008**, *47*, 7908–7913.

[13] a) K. Shiren, S. Ogo, S. Fujinami, H. Hayashi, M. Suzuki, A. Uehara, Y. Watanabe, Y. Moro-oka, *J. Am. Chem. Soc.* **2000**, *122*, 254–262; b) S. Itoh, H. Bandoh, M. Nakagawa, S. Nagatomo, T. Kitagawa, K. D. Karlin, S. Fukuzumi, *J. Am. Chem. Soc.* **2001**, *123*, 11168–11178; c) S. Hikichi, M. Yoshizawa, Y. Sasakura, H. Komatsuzaki, Y. Moro-oka, M. Akita, *Chem. Eur. J.* **2001**, *7*, 5011–5028; d) S. Itoh, H. Bandoh, S. Nagatomo, T. Kitagawa, S. Fukuzumi, *J. Am. Chem. Soc.* **1999**, *121*, 8945–8946; e) R. Schenker, B. S. Mandimutsira, C. G. Riordan, T. C. Brunold, *J. Am. Chem. Soc.* **2002**, *124*, 13842–13855; f) K. Fujita, R. Schenker, W. Gu, T. C. Brunold, S. P. Cramer, C. G. Riordan, *Inorg. Chem.* **2004**, *43*, 3324–3326.

[14] S. Kundu, F. F. Pfaff, E. Miceli, I. Zaharieva, C. Herwig, S. Yao, E. R. Farquhar, U. Kuhlmann, E. Bill, P. Hildebrandt, H. Dau, M. Driess, C. Limberg, K. Ray, *Angew. Chem. Int. Ed.* **2013**, *52*, 5622–5626; *Angew. Chem.* **2013**, *125*, 5732–5736.

[15] a) D. Huang, R. H. Holm, *J. Am. Chem. Soc.* **2010**, *132*, 4693–4701; b) D. Huang, O. V. Makhlynets, L. L. Tan, S. C. Lee, E. V. Rybak-Akimova, R. H. Holm, *Proc. Natl. Acad. Sci. USA* **2011**, *108*, 1222–1227; c) D. Huang, O. V. Makhlynets, L. L. Tan, S. C. Lee, E. V. Rybak-Akimova, R. H. Holm, *Inorg. Chem.* **2011**, *50*, 10070–10081; d) O. Troeppner, D. Huang, R. H. Holm, I. Ivanović-Burmazović, *Dalton Trans.* **2014**, *43*, 5274–5279.

[16] A. K. Patra, R. Mukherjee, *Inorg. Chem.* **1999**, *38*, 1388–1393.

[17] a) P. J. Donoghue, A. K. Gupta, D. W. Boyce, C. J. Cramer, W. B. Tolman, *J. Am. Chem. Soc.* **2010**, *132*, 15869–15871; b) P. Pirovano, A. M. Magherusan, C. McGlynn, A. Ure, A. Lynes, A. R. McDonald, *Angew. Chem. Int. Ed.* **2014**, *53*, 5946–5950; *Angew. Chem.* **2014**, *126*, 6056–6060.

[18] M. R. Halvagar, P. V. Solntsev, H. Lim, B. Hedman, K. O. Hodgson, E. I. Solomon, C. J. Cramer, W. B. Tolman, *J. Am. Chem. Soc.* **2014**, *136*, 7269–7272.

[19] F. A. Bell, A. Ledwith, D. C. Sherrington, *J. Chem. Soc. C* **1969**, 2719–2720.

[20] N. G. Connelly, W. E. Geiger, *Chem. Rev.* **1996**, *96*, 877–910.

[21] a) A. G. Lappin, M. C. M. Laranjeira, R. D. Peacock, *Inorg. Chem.* **1983**, *22*, 786–791; b) S. A. Jacobs, D. W. Margerum, *Inorg. Chem.* **1984**, *23*, 1195–1201; c) H. J. Kruger, R. H. Holm, *J. Am. Chem. Soc.* **1990**, *112*, 2955–2963; d) H. J. Kruger, G. Peng, R. H. Holm, *Inorg. Chem.* **1991**, *30*, 734–742; e) J. M. Corker, J. Evans, W. Levason, M. D. Spicer, P. Andrews, *Inorg. Chem.* **1991**, *30*, 331–334; f) T. Storr, P. Verma, Y. Shimazaki, E. C. Wasinger, T. D. P. Stack, *Chem. Eur. J.* **2010**, *16*, 8980–8983; g) Y.-M. Lee, S. Hong, Y. Morimoto, W. Shin, S. Fukuzumi, W. Nam, *J. Am. Chem. Soc.* **2010**, *132*, 10668–10670; h) T.-P.-A. Cao, G. Nocton, L. Ricard, X. F. Le Goff, A. Auffrant, *Angew. Chem. Int. Ed.* **2014**, *53*, 1368–1372; *Angew. Chem.* **2014**, *126*, 1392–1396.

[22] a) F. V. Lovecchio, E. S. Gore, D. H. Busch, *J. Am. Chem. Soc.* **1974**, *96*, 3109–3118; b) R. I. Haines, A. McAuley, *Coord. Chem. Rev.* **1981**, *39*, 77–119; c) J. N. Stuart, A. L. Goerges, J. M. Zaleski, *Inorg. Chem.* **2000**, *39*, 5976–5984.

[23] a) R. I. Haines, A. Mcauley, *Inorg. Chem.* **1980**, *19*, 719–723; b) P. J. Alonso, L. R. Falvello, J. Forniés, A. Martín, B. Menjón, G. Rodríguez, *Chem. Commun.* **1997**, 503–504; c) T. J. Collins, T. R. Nichols, E. S. Uffelman, *J. Am. Chem. Soc.* **1991**, *113*, 4708–4709; d) X. Ottenwaelder, R. Ruiz-García, G. Blondin, R. Carasco, J. Cano, D. Lexa, Y. Journaux, A. Aukauloo, *Chem. Commun.* **2004**, 504–505.

[24] a) G. J. Colpas, M. J. Maroney, C. Bagyinka, M. Kumar, W. S. Willis, S. L. Suib, P. K. Mascharak, N. Baidya, *Inorg. Chem.* **1991**, *30*, 920–928; b) J. Cho, H. Y. Kang, L. V. Liu, R. Sarangi, E. I. Solomon, W. Nam, *Chem. Sci.* **2013**, *4*, 1502–1508.

[25] a) M. Haumann, A. Porthun, T. Buhrke, P. Liebisch, W. Meyer-Klaucke, B. Friedrich, H. Dau, *Biochemistry* **2003**, *42*, 11004–11015; b) G. Davidson, S. B. Choudhury, Z. Gu, K. Bose, W. Roseboom, S. P. J. Albracht, M. J. Maroney, *Biochemistry* **2000**, *39*, 7468–7479; c) R. Sarangi, *Coord. Chem. Rev.* **2013**, *257*, 459–472.

[26] T. Schaefer, J. Schindelka, D. Hoffmann, H. Herrmann, *J. Phys. Chem. A* **2012**, *116*, 6317–6326.

[27] M. S. Alnajjar, X.-M. Zhang, G. J. Gleicher, S. V. Truksa, J. A. Franz, *J. Org. Chem.* **2002**, *67*, 9016–9022.

[28] a) E. R. Altwicker, *Chem. Rev.* **1967**, *67*, 475–531; b) J. M. Wittman, R. Hayoun, W. Kaminsky, M. K. Coggins, J. M. Mayer, *J. Am. Chem. Soc.* **2013**, *135*, 12956–12959.

[29] a) C. V. Sastri, M. J. Park, T. Ohta, T. A. Jackson, A. Stubna, M. S. Seo, J. Lee, J. Kim, T. Kitagawa, E. Münck, L. Que, W. Nam, *J. Am. Chem. Soc.* **2005**, *127*, 12494–12495; b) J. England, M. Martinho, E. R. Farquhar, J. R. Frisch, E. L. Bominaar, E. Münck, L. Que, *Angew. Chem. Int. Ed.* **2009**, *48*, 3622–3626; *Angew. Chem.* **2009**, *121*, 3676–3680.

[30] T. Kurahashi, A. Kikuchi, Y. Shiro, M. Hada, H. Fujii, *Inorg. Chem.* **2010**, *49*, 6664–6672.

Received: December 15, 2014

FULL PAPER

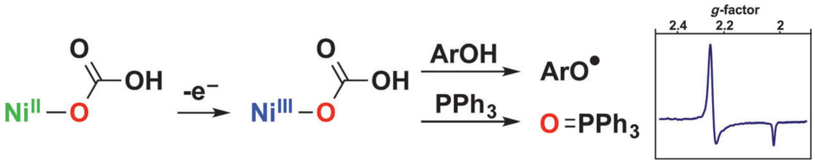

A nickel(III)–bicarbonate complex is obtained in high yield by the oxidation of a nickel(II) precursor. The nickel(III) species readily performs hydrogen atom abstraction and oxygen atom transfer at low temperatures, demonstrating that it is a viable model for elusive high-valent terminal nickel–oxygen intermediates in oxidation catalysis.

Metal–Oxo Species

*P. Pirovano, E. R. Farquhar, M. Swart, A. J. Fitzpatrick, G. G. Morgan, A. R. McDonald**

■■ – ■■

Characterization and Reactivity of a Terminal Nickel(III)–Oxygen Adduct